G-Tech : Jurnal Teknologi Terapan
Vol. 9, No. 2, 2025, p. 769-778
E-ISSN: 2623-064X | P-ISSN: 2580-8737

Analysis of Overcurrent Protection on Nuri Feeder of Yarmokh PLTD Due to Short Circuit

Ekawati Margaretha Ohee [1]✉, Yakobus[2], Oktavianus Kati[3], Dultudes Mangopo[4]

[1, 2, 3, 4] Department of Electrical Engineering, Faculty of Engineering, Universitas Cenderawasih, Indonesia

✉ **Corresponding Author :** Ekawati Margaretha Ohee (e-mail: oheeekawati@gmail.com)

Article Information

Article History

Received : February 05, 2025
Revised : March 12, 2025
Published : April 10, 2025

***Keywords*:**

Overcurrent relay coordination;
Power distribution network;
Short-circuit current;
Time Multiplier Settings (TMS);
Transmission lines

ABSTRACT

Protection systems are security mechanisms designed to safeguard electrical equipment from technical malfunctions, natural disturbances, operational errors, and other causes. These systems serve as electrical safety measures in power systems installed in power distribution networks, power transformers, electric power transmission lines, and generators, all of which protect the electrical system from faults or overloads. This research aimed to determine the short-circuit current and the overcurrent relay settings for the Nuri feeder at PLTD Yarmork. The method employed in this study involved collecting primary data directly from the field through observation and load measurements on transformers and distribution network lengths, followed by manual calculations. The research findings indicated that the maximum short-circuit current resulting from a three-phase fault at a fault location of 0% along the feeder was 6978.448 A, while the minimum current at 100% was 2313.838 A. For two-phase faults, the maximum short-circuit current at 0% feeder length was 976043.513 A, and the minimum current at 100% feeder length was 2003.842 A. The calculated TMS settings were 0.147 for the outgoing side of the OCR and 0.270 for the incoming side. Overall, the computed settings for both the overcurrent and earth fault relays were aligned with the field settings.

INTRODUCTION

Overcurrent protection is vital for electrical distribution systems against short-circuit interference (Nikolaidis et al., 2016; Pham et al., 2023). In traditional radial distribution systems, it is conventionally executed via a feeder recloser, coordinated with an overcurrent relay and downstream fuse (Nikolaidis et al., 2016). Nonetheless, the incorporation of distributed generation (DG) significantly alters short-circuit current characteristics, challenging traditional protection methods (Motabarian et al., 2013; Pham et al., 2023; Thararak & Jirapong, 2020).

To mitigate these challenges, advanced current protection strategies have been proposed in scholarly discourse. One method involves communications-assisted over-current protection, where devices share information regarding network configuration and short-circuit levels to dynamically modify their settings (Nikolaidis et al., 2016; Schaefer et al., 2010; Zamani et al., 2012). This adaptation enables the protection scheme to consider the implications of DG integration on network dynamics.

Another method involves the utilization of directional current relays for enhanced selective protection against interference current flow (Ehrenberger, 2015; Jones & Kumm, 2014; Serna &

This is an open access article under the CC BY license

López-Lezama, 2018). This is crucial in distribution networks characterized by bidirectional power flow due to distributed generation (DG) (Pham et al., 2023; Thararak & Jirapong, 2020). Directional current relays can be effectively coordinated to facilitate selective disconnection at the affected section while ensuring backup protection (Ehrenberger, 2015; Jones & Kumm, 2014; Serna & López-Lezama, 2018).

To enhance overcurrent protection performance in the presence of DG, various studies advocate for the implementation of interference current limiters, including superconducting interference current limiters (SFCL), to manage short-circuit current levels (Motabarian et al., 2013; Park et al., 2011). SFCLs may be integrated within protection coordination frameworks to guarantee optimal relay functionality (Motabarian et al., 2013; Park et al., 2011).

Additionally, adaptive protection schemes have been established, wherein current protection settings are continually refined based on real-time system parameter measurements, such as load conditions and short-circuit current levels (Abdullah Asuhaimi bin Mohd Zin & Shariati, 2015; Coffele et al., 2015; Schaefer et al., 2010). This adaptability enables protection systems to respond effectively to variations in network topology and DG integration (Abdullah Asuhaimi bin Mohd Zin & Shariati, 2015; Coffele et al., 2015; Schaefer et al., 2010).

For microgrids, which possess the capability to function in both grid-connected and islanded configurations, the challenges associated with protection mechanisms are significantly exacerbated by the variable short-circuit current contributions arising from Distributed Generation (DG) units (Gkountaras et al., 2015; Thararak & Jirapong, 2020). In this context, a communications-based adaptive protection framework, which adheres to the IEC 61850 standard, has been advocated to ensure both reliable and selective protective measures across the aforementioned operational modes (Memon & Kauhaniemi, 2020).

The causative factors of short circuits include failures in isolation, external disturbances, or operational inaccuracies. A meticulous analysis of the efficacy of existing overcurrent protection systems, encompassing protection relays and additional safety devices, is imperative for the detection and isolation of short circuits, aimed at mitigating potential damage (Firmansyah et al., 2022; Paithankar, 2017). Furthermore, it is essential to provide recommendations for enhancements or refinements of overcurrent protection systems grounded in the conducted analysis, with the objective of elevating the reliability and safety of the electric power infrastructure. This rationale underpins the authors' investigation into the calibration of overcurrent protection mechanisms in response to short circuit occurrences at the Yarmokh PLTD Nuri Repeater. Drawing on data from PT PLN (Persero) Jayapura, it is evident that the Nuri PLTD generator at Yarmokh is subjected to a substantial load of 4300 kWh, resulting in a significant trip percentage for the repeater; thus, it is necessary to undertake calculations for the adjustment of the overcurrent relay.

METHOD

The investigation was executed at the Skyline Jayapura Substation (GI), focusing on the assessment of overcurrent protection within the Nuri PLTD Yarmokh repeater under conditions of short circuit. The analysis of load protection employs a predominantly manual computational methodology, utilizing pertinent equations to evaluate the efficacy of the system. Initially, the single line diagram of the Nuri repeater was meticulously scrutinized to gain insights into the network configuration, thereby establishing a foundational framework for delineating the essential components and their interconnections within the electrical system.

Moreover, the compilation and application of various data, encompassing power transformer capacity, voltage specifications, physical lengths of conductors and channels, as well as transformer impedance (as illustrated in Table 1), were undertaken. Each of these parameters was diligently measured and computed manually, employing equations tailored to the electrical characteristics of the system (as depicted in Figure 1).

Table 1. Power transformer and conductor specifications.

Deskripsi	Uraian
Merk	UNINDO
Type	Step Down – Powet Transformator
Power	60 MVA
Voltage	150 kV
Impedance	12,82%
Primary Voltage	150 kV
Secondary Voltage	20 kV
CT Ratio	2000/5
Nominal Transformer	1574,6 A
Rating Winding Configuration	Ynyn0rd
Ground Resistance	12 Ohm

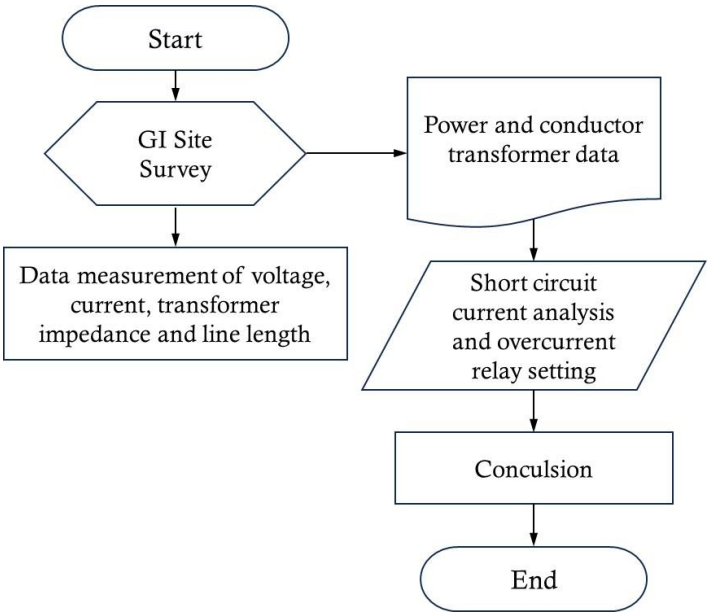

Figure 1. Research process flow

The ensuing computational methodology facilitates the exact quantification of interference currents alongside the pertinent thresholds for over-current protection apparatuses, thereby guaranteeing that the safety mechanisms of the system are meticulously calibrated (Nursalim et al., 2019).

RESULTS AND DISCUSSION

Short Circuit Interruption

1) 1Current Source Impedance

The Short Circuit data pertaining to the primary side bus (150 kV) at the Skyline substation indicates a capacity of 500 MVA; consequently, the source impedance (XS) is:

$$XS\ (sisi\ 150\ kV) = \frac{kV\ (primary\ side\ of\ the\ transformer)}{MVA\ (short\ circuit\ in\ the\ primary\ side\ bus)}$$

$$= \frac{150^2}{500} = 45\ ohm$$

$$Xs\ (sisi\ 20\ kV) = \frac{kV\ (the\ secondary\ side\ of\ the\ transformer)^2}{kV(the\ primary\ side\ of\ the\ transformer)^2} \times Xs\ (the\ primary\ side) ohm$$

$$= \frac{20^2}{150^2} \times 45 = 0{,}8\ ohm$$

2) Transformer Reactance

The Skyline Substation exhibits a transformer reactance of 12.82%. In order to ascertain the magnitude of the reactance values corresponding to the positive sequence and the zero sequence in ohmic terms, it is imperative to initially compute the value of the electric current at the nominal 100% position, as delineated below (Setyaningrum et al., 2021):

$$Xt\ (at\ 100\%) = \frac{kV^2 sisi\ bus^2}{MVA\ trafo}$$

$$Xt\ (at\ 100\%) = \frac{20^2}{60} = 6{,}667\ ohm$$

The reactance characteristics of the power transformer, which comprise both positive sequence reactance and zero sequence reactance, are delineated as follows:

Positive and negative sequence reactance ($Xt_1 = Xt_2$)

$$Xt = 12{,}82\% \times 6{,}667$$

$$= 0{,}8547$$

The zero-sequence reactance for the Skyline Substation Transformer, exhibiting a Ynyn0 configuration devoid of any delta winding, indicates that the magnitude of Xt_0 varies within the range of 9 to 14. In this analytical discourse, the author posits the value of Xt_1 to be calculated as Xt_0 minus 10 Xt_1.

So, $Xt_0 = 10 \times 0{,}8547$

$= 8{,}5467\ ohm$

3) Repeater Impedance

According to the information acquired from the regional office, it has been established that the specific type of conductor employed in the Nuri Repeater is AAAC 150 mm2, and the total length of the repeater measures 8.92 kilometers; consequently, the impedance associated with the Nuri Repeater is (Galla et al., 2020):

$$Z_1 = Z_2(AAAC\ 150\ mm^2) = (0{,}2162 + J\ 0{,}3305) \times 8{,}92$$

$$= 1{,}9285 + J\ 2{,}9481$$

$$Z_0(AAAc\ 150) = (0{,}3631 + J\ 1{,}6180) \times 8{,}92$$

$$= 3{,}2389 + J\ 14{,}4326$$

Consequently, the impedance values associated with repeaters at distances of 0%, 25%, 50%, 75%, and 100% of their respective lengths are delineated in Table 2.

Table 2. Positive and negative sequence impedance of feeder (Z_1Z_2)

% Lenght	Repeater Impedance (Z1 and Z2)	Result
0	0% x (1,9285 + *j* 2,9481)	0
25	25% x (1,9285 + *j* 2,9481)	0,4821 + *j* 0,7370
50	50% x (1,9285 + *j* 2,9481)	0,9643 + *j* 1,4740
75	75% x (1,9285 + *j* 2,9481)	1,4464 + *j* 2,2110
100	100% x (1,9285 + *j* 2,9481)	1,9285 + *j* 2,9481

4) Equivalent Network Impedance

The subsequent expression delineates the equivalent impedance of the network, specifically (Jeschke et al., 2023):

$$Z_{1eq} = Z_{2eq} \quad = Z_1 s\ (sisi\ 20\ kV) + Z_{iT} + Z_1\ repeater$$
$$= J\ 0{,}8 + J\ 0{,}8547 + Z_1\ repeater$$
$$= J\ 1{,}6547 + Z_1\ repeater$$

Given that the locus of the interference is posited to be at 0%, 25%, 50%, 75%, and 100% of the length of the repeater, the resultant Z1 eq (Z2 eq) is as follows:

Table 3. Equivalent Impedance ($Z_{1\ eq}$, $Z_{2\ eq}$)

% Lenght	Repeater Impedance (Z1 and Z2)	Result
0	(j 1,6547+ 0)	0 + + j 1,6547
25	25% x (1,9285 + j 1,6547+ j 0,7370)	0,4821 + j 2,3917
50	50% x (1,9285 + j 1,6547+ j 1,4740)	0,9643 + j 3,1287
75	75% x (1,9285 + j 1,6547+ j 2,2110)	1,4464 + j 3,8657
100	100% x (1,9285 + j 1,6547+ j 2,9481)	1,9285 + j 4,6027

Short Circuit Interruption Current

1) 3-phase Short Circuit Interruption

$$I = \frac{V}{Z}$$

Where, I = represents the three-phase interference current; V denotes the phase voltage in a neutral system, quantified as 20 kV=20000/√3 ph; and Z signifies the positive sequence impedance ($Z_{_1eq}$).

$$I_3phase = \frac{Vph}{Z_{ieq}} = \frac{20.000}{\sqrt{3}}$$

$$I_3phase = \frac{11.547{,}00538379}{Z_{ieq}}$$

Tabel 4. 3 phase short circuit fault current

% Lenght	Fault current (A)
0	6978,448
25	4732,782
50	3526,971
75	2797,621
100	2313,838

2) 2-phase Short Circuit Interruption

$$I = \frac{V}{S}$$

Where, I represents the interference current associated with a two-phase short-circuit; V denotes the phase voltage of a 20 kV electrical system; and Z signifies the aggregate of positive sequence impedances (Z_{ieq}) and negative sequence impedances (Z_{0eq}).

In this context, the relationship Z_{1eq} = Z_{2eq} holds true. Consequently, the previously mentioned equation for the two-phase short-circuit interference current can be articulated in a more simplified manner as follows:

$$I_2 fasa = \frac{vph-ph}{2 \times Z_1\, eq} = \text{I}_{\text{3fasa}} \times 0{,}8666$$

Table 5. 2 phase short circuit fault current

% Lenght	Fault current (A)
0	6043,511
25	4098,709
50	3054,446
75	2422,811
100	2003,842

Overcurrent Relay Configurations

In accordance with the aforementioned Table 4 and Table 5, it is evident that the short-circuit interference current is influenced by the spatial distance from the interference point; specifically, as the interference point is positioned further from the busbar, the magnitude of the interference current diminishes. Conversely, it can be observed that the proximity of the disturbance point to the busbar results in an amplified disturbance current.

1) Overcurrent relay configuration on the outgoing side of the 20 kV repeater

Subsequent to the installation of the relay within the repeater, the settings are determined based on the load current. For relays exhibiting normal inverse characteristics, the configuration is established at 1.05 to 1.3 times the load current (load). Additionally, a critical criterion that must be adhered to is the stipulation that the setting shall not be less than 0.3 seconds.

$$\text{I}_{\text{beban}} = 240 \text{ A; CT} = 300/5 \text{ A}$$

$$\text{I}_{\text{set (primer)}} = 1{,}05 \text{ x I}_{\text{beban}}$$

$$= 1,\ 05 \text{ x } 240$$

$$= 252 \text{ A}$$

The instantaneous value pertains to the designated value on the primary side; to derive the secondary setting value that is to be configured on the relay, it is imperative to perform calculations utilizing the parameters of the current transformer ratio integrated within the outgoing feeder. The secondary current setting can be computed as delineated below:

$$\text{I}_{\text{sekunder}} = I_{set\ (primer)} \times \frac{1}{Ratio\ CT}$$

$$= 252 \times \frac{5}{300}$$

$$= 4{,}2 \text{ A}$$

2) TMS Setting for the Overcurrent Relay on the Outgoing Side of the 20 kV Repeater

To ascertain the value of the time multiplier setting (TMS) on the overcurrent relay (OCR) associated with the 20 kV repeater, the short-circuit fault current (Ifault) is employed, which represents a three-phase current at 0% of the repeater's capacity. The operational response time (t) for the designated overcurrent setting (OCR) is established at t = 0.3 seconds.

This particular choice was made to prevent the relay from tripping in response to the inrush current generated by the distribution transformers already integrated into the distribution network at the moment the primary metering transformer (PMT) of the repeater is engaged.

$$tms = \frac{t \times \left[\left\{\frac{Ifault}{Iset(primer)}\right\}^{0{,}02} - 1\right]}{0{,}14}$$

$$tms = \frac{0{,}3 \times \left[\left\{\frac{6978{,}4481}{252}\right\}^{0{,}02} - 1\right]}{0{,}14}$$

$$tms = 0{,}147$$

3) Overcurrent Relay Configuration on the Incoming Side at 20 kV

Based on the collected data, the capacity is determined to be 60 MVA; the voltage levels are 150/20 kV; the impedance is calculated at 12.82%; and the current transformer ratio is established at 600/5 A. Consequently, the nominal current of the transformer on the 20 kV side is

$$I_{nominal} = \frac{KVA\,Trafo}{KV\ (sisi\ 20)\times\sqrt{3}} \text{ x } 80\%$$

$$= \frac{60}{20\times\sqrt{3}}$$

$$= 1{,}732050808\ kA \times 0{,}8$$

$$= 1385{,}640 \text{ A}$$

$$I_{set\ primer} = 1{,}05 \times I_{load}$$

$$= 1{,}05 \times 480$$

$$= 504 \text{ A}$$

While the setting value on the secondary side is

$$I_{set\ (sekunder)} = I_{set\ primer} \times \frac{1}{Ratio\ CT}$$

$$= 504 \times \frac{5}{600}$$

$$= 4{,}2 \text{ A}$$

4) TMS Modification of the Incoming 20 kV

Overcurrent Relay Segment The interference current is designated to ascertain the intensity of the Time Multiplier Setting (TMS) for the Overcurrent Relay (OCR) associated with the Incoming 20 kV power transformer, which experiences a three-phase short-circuit interference current at 0% of the repeater length (Macieira & Coelho, 2017). The operational time for the incoming system is derived from the relay's operational time on the downstream segment, which is +0.4 seconds.

$$t_{incoming} = (0{,}3 + 0{,}4) = 0{,}7 \text{ second.}$$

So, obtained:

$$t = \frac{0{,}14\times tms}{\left[\frac{Ifault}{I\,set}\right]^{0{,}02} - 1}$$

$$0{,}7 = \frac{0{,}14\times tms}{\left[\frac{6976{,}45}{504}\right]^{0{,}02} - 1}$$

$$TMS = 0{,}270$$

Relay Operational Time Assessment

The operational duration of the relay must be evaluated in relation to the intensity of the interference current at various interference thresholds of 0%, 25%, 50%, 75%, and 100% in order to ascertain the functionality of the relay.

1) Setting the operational time of the relay (t) during a three-phase fault condition

The operational duration of the relay at the fault locus on the 0% side of both the outgoing and incoming feeder at a voltage of 20 kV is recorded as 0.300 seconds and 0.700 seconds, respectively. Additional data regarding other disturbance locations can be referenced in Table 6.

Table 6. Temporal configuration of the three-phase overcurrent relay

% Lenght	Fault current (A)	Incoming relay time (seconds)	Outgoing relay time (seconds)
0	6978,448	0,300	0,700
25	4732,782	0,341	0,825
50	3526,971	0,380	0,952
75	2797,621	0,418	1,083
100	2313,838	0,454	1,221

2) Establishing the operational duration of the relay (t) during a 2-phase breakdown

The operational duration of the relay, when subjected to interference on the 0% margin of both the outgoing and incoming repeater at a voltage level of 20 kV, is recorded at 0.314 seconds and 0.742 seconds, respectively. Additional data concerning other 2-phase perturbation positions is available in Table 7.

Table 7. Temporal configuration of the two phase overcurrent relay

% Lenght	Fault current (A)	Incoming relay time (seconds)	Outgoing relay time (seconds)
0	6043,511	0,314	0,742
25	4098,709	0,359	0,882
50	3054,446	0,403	1,030
75	2422,811	0,445	1,184
100	2003,842	0,487	1,350

The data obtained from the review of the overcurrent relay's adjustment value is critical in understanding the degree of short-circuit interference current relative to the distance from the source of disturbance; specifically, as one distances themselves from the interference source, the short-circuit interference current becomes weaker, while being close to the disturbance point increases the short-circuit interference current's level. Furthermore, it becomes evident that the distance of the interference location significantly influences the magnitude of the time differential; as the distance to the interference increases, the time differential becomes less pronounced, particularly when comparing the operational duration of the repeater relay to that of the incoming relay and so forth. In the event that the relay on the repeater side fails to provide adequate protection, the relay on the incoming side will immediately engage as a safety backup; moreover, the operational duration of the relay is also contingent upon the magnitude of the interference current, where an increase in the interference current correlates with a more rapid relay operation. Upon executing the calculations for the Time Multiplier Setting (TMS) of the overcurrent relay (OCR) on both the outgoing and incoming sides, a comparative analysis with the empirical data observed in the field is illustrated in Table 8.

Table 8. Comparison of calculation results with field data

Relay name	Calculation results		Field data	
	I_{set} primer (A)	TMS	I_{set} primer (A)	TMS
Outgoing vercurrent	252	0,417	300	0,05
Incoming overcurrent	504	0,270	600	0,23

The computed outcomes reveal that the peak three-phase short-circuit current reaches 6978.448 A at 0% of the feeder length, diminishing to 2313.838 A at 100%, while two-phase fault currents demonstrate a comparable declining pattern. The data corroborates prior findings, particularly those of Nikolaidis et al. (2016) and Coffele et al. (2015), showing a substantial drop in fault current levels as the fault's location is displaced from the source, a factor linked to the escalation in feeder impedance. The established Time Multiplier Settings (TMS) of 0.147 for the outgoing section and 0.270 for the incoming section also conform to global standards and recent scholarly contributions, including studies by Pham et al. (2023) and Thararak and Jirapong (2020), highlighting the imperative for differential relay sensitivity to accommodate fluctuating fault currents along the feeder. Furthermore, the suggestion to adjust the primary current setting based on actual load circumstances rather than exclusively on the maximum CT rating is bolstered by research from Motabarian et al. (2013) and Macieira and Coelho (2017), which advocate for adaptive protection mechanisms in contemporary distribution networks. These comparisons with international literature and recognized standards reinforce the robustness of the analysis and highlight the practical significance of optimizing relay settings to improve system protection efficacy.

CONCLUSION

The calculated relay settings have significant implications for system protection performance. The maximum short-circuit current induced by three-phase interference at the most critical disturbance location (0% of the repeater length) is 6978.448 A, decreasing to 2313.838 A at 100% of the repeater length. Conversely, the short-circuit current from two-phase interference is 976043.513 A at 0% and drops to 2003.842 A at 100%, clearly demonstrating that the closer the interference, the higher the disturbance current. The computed Time Multiplier Settings (TMS) are 0.147 for the outgoing side and 0.270 for the incoming side, indicating a need for differential relay sensitivity. To optimize protection performance, the primary current setting for the outgoing side should be calibrated not to the maximum rating of the installed CT but rather to the repeater's load current under peak conditions, adjusted by a multiplication factor in accordance with standard inverse timing settings.

ACKNOWLEDGEMENTS

Thank you for the cooperation of friends who have contributed to the research and preparation of this journal manuscript. Also to the leaders who have provided support for facilities and infrastructure during the implementation of data collection.

REFERENCES

Abdullah Asuhaimi bin Mohd Zin, & Shariati, O. (2015). *On-Line Overcurrent Relays Setting Approach in Distribution Networks by Implementing New Adaptive Protection Algorithm*. https://doi.org/10.1109/issnip.2015.7106960

Coffele, F., Booth, C., & Dyśko, A. (2015). An Adaptive Overcurrent Protection Scheme for Distribution Networks. *Ieee Transactions on Power Delivery*, *30*(2), 561–568. https://doi.org/10.1109/tpwrd.2013.2294879

Ehrenberger, J. (2015). *Use of Directional Overcurrent Protection Scheme for Distributed Generation Systems*. https://doi.org/10.1109/epe.2015.7161082

Firmansyah, A., Suyadi, A., & Satriaoktarian, M. B. (2022). Unjuk Kerja Over Current Relay Pada Incoming dan Outgoing Transformer Daya #1 60 MVA Gardu Induk Kenten menggunakan ETAP 19.0.1. *Jurnal Tekno*, *19*(1), 01–10. https://doi.org/10.33557/jtekno.v19i1.1613

Galla, W. F., Sampeallo, A. S., & Daris, J. I. (2020). Analisis Gangguan Hubung Singkat Pada Saluran Udara 20 KV Di Penyulang Naioni PT. PLN (Persero) ULP Kupang Untuk Menentukan Kapasitas Pemutusan Fuse Cut Out Menggunakan ETAP 12.6. *Jurnal Media Elektro*, 101–112. https://doi.org/10.35508/jme.v0i0.3208

Gkountaras, A., Dieckerhoff, S., & Sezi, T. (2015). *Development of a Short Circuit Strategy for Medium Voltage Hybrid Microgrids*. https://doi.org/10.1109/pedg.2015.7223020

Jeschke, S., Olbrich, M., Kleinen, M., & Baerenfaenger, J. (2023). Development of a Equivalent Impedance Network Reproducing the Impedance of Electric Vehicles During Active DC Charging. *2023 IEEE Vehicle Power and Propulsion Conference (VPPC)*, 1–5. https://doi.org/10.1109/VPPC60535.2023.10403257

Jones, D., & Kumm, J. (2014). Future Distribution Feeder Protection Using Directional Overcurrent Elements. *Ieee Transactions on Industry Applications*, *50*(2), 1385–1390. https://doi.org/10.1109/tia.2013.2283237

Macieira, G. L., & Coelho, A. L. M. (2017). Evaluation of numerical time overcurrent relay performance for current transformer saturation compensation methods. *Electric Power Systems Research*, *149*, 55–64. https://doi.org/10.1016/j.epsr.2017.04.005

Memon, A. A., & Kauhaniemi, K. (2020). An Adaptive Protection for Radial AC Microgrid Using IEC 61850 Communication Standard: Algorithm Proposal Using Offline Simulations. *Energies*, *13*(20), 5316. https://doi.org/10.3390/en13205316

Motabarian, F., Golkar, M. A., & Hajiaghasi, S. (2013). *Surveying the Effect of Distributed Generation (DG) on Over Current Protection in Radial Distribution Systems*. 1–6. https://doi.org/10.1109/epdc.2013.6565955

Nikolaidis, V. C., Papanikolaou, E., & Safigianni, A. (2016). A Communication-Assisted Overcurrent Protection Scheme for Radial Distribution Systems With Distributed Generation. *Ieee Transactions on Smart Grid*, *7*(1), 114–123. https://doi.org/10.1109/tsg.2015.2411216

Nursalim, N., Sampeallo, A. S., & Willi, A. P. L. (2019). Analisis Koordinasi Dan Setting Over Current Relay (OCR) Pada Pemakaian Daya Sendiri PLTU SMS Energy Menggunakan Software ETAP 12.6.0. *Jurnal Media Elektro*, 100–109. https://doi.org/10.35508/jme.v0i0.1884

Paithankar, Y. G. (2017). Line Protection: Overcurrent and Directional Relays. In Y. G. Paithankar, *Transmission Network Protection* (1st ed., pp. 25–74). Routledge. https://doi.org/10.1201/9780203735176-3

Park, W., Sung, B. C., Song, K., & Park, J. (2011). Parameter Optimization of SFCL With Wind-Turbine Generation System Based on Its Protective Coordination. *Ieee Transactions on Applied Superconductivity*, *21*(3), 2153–2156. https://doi.org/10.1109/tasc.2010.2090855

Pham, L. N. H., Wagle, R., & González-Longatt, F. (2023). *Concise Definition of the Overcurrent Protection System for CIGRE European Medium Voltage Benchmark Network*. 1–5. https://doi.org/10.1109/isgtmiddleeast56437.2023.10078621

Schaefer, N., Degner, T., Shustov, A., Keil, T., & Jaeger, J. (2010). *Adaptive Protection System for Distribution Networks With Distributed Energy Resources*. P69–P69. https://doi.org/10.1049/cp.2010.0344

Serna, J. J., & López-Lezama, J. M. (2018). An Alternative Method for Obtaining the Optimal Directional Characteristic Angle of Directional Overcurrent Relays in Transmission Networks. *Contemporary Engineering Sciences*, *11*(4), 149–164. https://doi.org/10.12988/ces.2018.8111

Setyaningrum, Y., Prasetyono, S., & Setiawan, A. (2021). Optimasi Koordinasi Over Current Relay Pada Trafo 60 MVA 150/20 KV dan Penyulang 20 KV Gumul Gardu Induk Banaran Berbasis Particle Swarm Optimization. *Jurnal Arus Elektro Indonesia*, *7*(1), 1. https://doi.org/10.19184/jaei.v7i1.21480

Thararak, P., & Jirapong, P. (2020). Implementation of Optimal Protection Coordination for Microgrids With Distributed Generations Using Quaternary Protection Scheme. *Journal of Electrical and Computer Engineering*, *2020*, 1–13. https://doi.org/10.1155/2020/2568652

Zamani, M. A., Yazdani, A., & Sidhu, T. S. (2012). A Communication-Assisted Protection Strategy for Inverter-Based Medium-Voltage Microgrids. *IEEE Transactions on Smart Grid*, *3*(4), 2088–2099. https://doi.org/10.1109/TSG.2012.2211045